

Mapping Star Formation Quenching Efficiency Across Feedback and Cosmological Parameter Space with CAMELS Simulations

ASTROPILOT¹

¹*Anthropic, Gemini & OpenAI servers. Planet Earth.*

ABSTRACT

Understanding the mechanisms that halt star formation in galaxies, leading to their eventual quenching, is a fundamental problem in astrophysics. The challenge lies in disentangling the complex interplay between internal feedback processes, such as those driven by supernovae (SNe) and active galactic nuclei (AGN), and the influence of the larger cosmological environment. These processes are highly degenerate, making it difficult to isolate the specific drivers responsible for quenching. In this study, we address this challenge by systematically quantifying the impact of feedback and cosmological parameters on star formation quenching at $z = 0$. We leverage the CAMELS simulation suite, a unique collection of hydrodynamical simulations designed to vary key astrophysical and cosmological parameters independently. By analyzing the relationships between galaxy properties and these parameters, we disentangle the relative importance of SNe, AGN feedback, and cosmological factors in regulating star formation and determine how they correlate with the quenched fraction of galaxies. Our analysis provides predictive insights for galaxy evolution models and offers a theoretical framework for interpreting future observational surveys aimed at understanding the quenching phenomenon, ultimately providing valuable constraints on the underlying physical processes driving galaxy evolution.

Keywords: Galaxy evolution, Galaxy quenching, Cosmological parameters, N-body simulations, Regression

1. INTRODUCTION

Understanding the physical processes that govern the evolution of galaxies remains a central goal of modern astrophysics. Galaxies, as the primary repositories of stars, gas, and dark matter, exhibit a remarkable diversity in their properties, ranging from actively star-forming spirals to quiescent ellipticals with little to no ongoing star formation. A critical phase in the life cycle of a galaxy is the transition from an active star-forming state to a quenched state, where star formation is significantly suppressed or halted altogether. Elucidating the mechanisms that drive this quenching phenomenon is essential for a complete understanding of galaxy evolution and the formation of the diverse galaxy population we observe throughout cosmic history. This endeavor requires a synergistic approach, combining sophisticated theoretical models with detailed observational constraints.

The regulation of star formation in galaxies is a complex process influenced by a multitude of factors operating on different scales. Internal feedback processes, driven by supernovae (SNe) and active galactic nuclei (AGN), play a crucial role in shaping the gas content and

star formation activity of galaxies (Hopkins et al. 2011; Carr et al. 2022). Supernovae inject energy and momentum into the interstellar medium (ISM), potentially heating and expelling gas, thereby suppressing star formation (Hopkins et al. 2011; Carr et al. 2022). Similarly, AGN can release vast amounts of energy in the form of radiation and outflows, which can also heat or remove gas from the galaxy, leading to quenching. These internal feedback mechanisms are intricately linked to the properties of the galaxy itself, such as its stellar mass, morphology, and gas content.

Furthermore, the larger cosmological environment in which a galaxy resides also exerts a significant influence on its star formation history (Wijesinghe et al. 2012; Shi et al. 2023; Pérez-Millán et al. 2023). Factors such as halo mass, merger history, and the density of the surrounding cosmic web can affect the inflow of fresh gas into galaxies, which fuels star formation (Wijesinghe et al. 2012; Pérez-Millán et al. 2023). Environmental effects can also trigger morphological transformations, such as the formation of a bulge, which can stabilize gas against collapse and prevent star formation (Pérez-Millán et al. 2023). Disentangling the relative

importance of these internal and external factors, and understanding how they interact to determine a galaxy’s star formation history, presents a formidable challenge (Pérez-Millán et al. 2023; Mucesh et al. 2024).

The observed properties of galaxies, such as their stellar mass, morphology, and star formation rate, represent the integrated outcome of these complex interactions (Das et al. 2021; Li et al. 2024a). This makes it difficult to isolate the specific drivers responsible for quenching based solely on observational data. Moreover, the theoretical modeling of these processes is computationally intensive, demanding high-resolution simulations that accurately capture the relevant physics on a wide range of scales (Das et al. 2023; Subramanian et al. 2023). Such simulations must faithfully reproduce both the internal physics of galaxies and their interaction with the larger cosmological environment.

To address these challenges, we present a systematic study aimed at quantifying the impact of feedback and cosmological parameters on star formation quenching at $z = 0$ (Piotrowska et al. 2021). Our approach leverages the CAMELS (Cosmology and Astrophysics with Machine Learning Simulations) simulation suite, a unique collection of hydrodynamical simulations specifically designed to independently vary key astrophysical and cosmological parameters. The CAMELS suite encompasses both the IllustrisTNG and SIMBA models, enabling us to explore the effects of different subgrid physics implementations on quenching. By analyzing the relationships between galaxy properties and these parameters, we aim to disentangle the relative importance of SNe, AGN feedback, and cosmological factors in regulating star formation (Bluck et al. 2023; Kurinchi-Vendhan et al. 2024).

Our methodology involves a comprehensive analysis of the CAMELS simulation data, focusing on the quenched fraction of galaxies as a key indicator of quenching efficiency (Xie et al. 2024). We employ a binning strategy to stratify galaxies by stellar mass and then further subdivide them based on the values of the feedback and cosmological parameters (Xie et al. 2024). This allows us to isolate the effects of each parameter on the quenched fraction, while controlling for other factors (Xie et al. 2024). Furthermore, we utilize statistical modeling techniques, such as multivariate logistic regression, to quantify the dependence of quenching efficiency on these parameters and to identify potential correlations and interactions. We model the quenched status of a galaxy as a binary variable, dependent on the input parameters (Xie et al. 2024).

We derive several key metrics from our analysis, including the quenched fraction as a function of stellar

mass and feedback/cosmological parameters (Xie et al. 2024,?; Geha et al. 2024), as well as the median specific star formation rate (sSFR) in each bin. We estimate the uncertainties on these metrics using bootstrap resampling techniques, providing a robust assessment of the statistical significance of our results. Additionally, we perform partial correlation analysis to isolate the direct effects of each parameter on the quenched fraction, controlling for stellar mass and other parameters (Porrás-Valverde & Forbes 2024). This allows us to identify the most influential factors driving quenching.

To validate our findings, we employ k-fold cross-validation techniques to assess the robustness of our regression models (Narkedimilli et al. 2024). This ensures that our results are not driven by overfitting or sample variance. We also perform a series of robustness checks, repeating key analyses with alternative binning schemes and sSFR thresholds to confirm the stability of our conclusions (Martin & Mortlock 2024,?). These validation steps provide confidence in the reliability of our results and the generalizability of our findings (Narkedimilli et al. 2024; Martin & Mortlock 2024,?). We explore the parameter space and compare our findings to those of previous works to ensure our results are consistent with the current understanding of galaxy evolution (Stoppa et al. 2023).

Our analysis provides predictive insights for galaxy evolution models and offers a theoretical framework for interpreting future observational surveys aimed at understanding the quenching phenomenon (Schawinski et al. 2018). By quantifying the relative importance of different feedback and cosmological parameters, we can provide valuable constraints on the underlying physical processes driving galaxy evolution (Lapi et al. 2025). This will help improve the accuracy and predictive power of galaxy evolution models, allowing them to better reproduce the observed properties of galaxies across cosmic time (Li et al. 2024b). The results can be used to improve the theoretical models which inform the observational surveys, and the observational surveys that improve the theoretical models (Comparat et al. 2025).

In future work, we plan to extend our analysis to higher redshifts, exploring the evolution of quenching efficiency over cosmic time (Mao et al. 2022; Bravo et al. 2023). This will provide a more complete picture of the quenching process and its dependence on feedback and cosmological parameters (Dou et al. 2025). We also plan to investigate the role of different quenching mechanisms, such as morphological quenching and environmental quenching, in more detail (Mao et al. 2022; Ellison et al. 2024). This will involve analyzing the morphology and environment of galaxies in the CAMELS

simulations and correlating these properties with their star formation activity (Mao et al. 2022; Bravo et al. 2023; Ellison et al. 2024). Ultimately, this will lead to a more comprehensive understanding of the complex interplay between internal and external factors in regulating galaxy evolution.

2. METHODS

2.1. Data Acquisition and Preparation

The foundation of this study rests upon the CAMELS (Cosmological and Astrophysical Models for Extremely Luminous Sources) project, a suite of cosmological hydrodynamical simulations. We utilize the publicly available data, specifically the IllustrisTNG and SIMBA simulation sets, each comprising 1000 simulations with varying cosmological and astrophysical parameters. The CAMELS simulations are particularly well-suited for this analysis due to their systematic variation of key parameters, enabling a disentangling of the effects of feedback and cosmology on galaxy evolution.

We begin by acquiring the galaxy-level data from the CAMELS database. This data is stored in `parquet` format for efficient storage and retrieval. Specifically, we load two primary dataframes: `galaxies_full_optimal.parquet`, containing detailed information on individual galaxies within the simulations, and `catalog_params_optimal.parquet`, providing the corresponding cosmological and feedback parameter values for each simulation. These dataframes are read into memory using the `pandas` library in Python, leveraging the `read_parquet` function for optimized I/O performance.

The `galaxies_full_optimal.parquet` dataframe contains crucial information for each galaxy, including its star formation rate (SFR) and stellar mass (`M_star`). The `catalog_params_optimal.parquet` dataframe contains the six parameters that are varied across the CAMELS simulations: two parameters controlling the efficiency of supernova feedback (`A_SN1`, `A_SN2`), two parameters controlling the efficiency of AGN feedback (`A_AGN1`, `A_AGN2`), the matter density parameter (`Omega_m`), and the amplitude of the matter power spectrum (`sigma_8`) (Villaescusa-Navarro et al. 2022; Lee et al. 2024). Each simulation is uniquely identified by a `catalog_number`.

2.2. Calculation of Derived Quantities and Data Integration

Following data loading, we compute the specific star formation rate (sSFR) for each galaxy, defined as the ratio of the SFR to the stellar mass ($\text{sSFR} = \text{SFR} / M_{\text{star}}$) (Bauer et al. 2005). This quantity serves as

a key indicator of a galaxy’s star-forming activity. We then define a galaxy as “quenched” if its sSFR falls below a threshold of 10^{-11} yr^{-1} (Whitaker et al. 2017; Katsianis et al. 2020; Leslie et al. 2020). A boolean column is added to the galaxy dataframe, indicating whether each galaxy meets this quenching criterion.

To link galaxy-level properties with the corresponding simulation parameters, we merge the `catalog_params_optimal.parquet` dataframe onto the `galaxies_full_optimal.parquet` dataframe using the `catalog_number` as the common key. This ensures that each galaxy is associated with the correct values of `A_SN1`, `A_SN2`, `A_AGN1`, `A_AGN2`, `Omega_m`, and `sigma_8` from its parent simulation (Contardo et al. 2025). The merging operation is performed using the `merge` function in `pandas` (de Santi et al. 2025; Ivanov et al. 2025).

2.3. Binning Strategy for Parameter Space Exploration

To systematically explore the influence of stellar mass, feedback, and cosmological parameters on quenching, we employ a binning strategy. First, galaxies are divided into bins based on their stellar mass. We utilize logarithmic bins, specifically $\log(M_{\text{star}}/M_{\odot}) = [8.5-9.5]$, $[9.5-10.5]$, and $[10.5-11.5]$ (Porras-Valverde & Forbes 2024). These bins are chosen to ensure sufficient galaxy counts within each bin, providing robust statistical analysis.

Within each stellar mass bin, we further stratify galaxies based on the feedback and cosmological parameters (Vaughan et al. 2024). For the feedback parameters (`A_SN1`, `A_SN2`, `A_AGN1`, `A_AGN2`) and the cosmological parameters (`Omega_m`, `sigma_8`), we divide their respective ranges into quantiles (Arango-Toro et al. 2025). This approach ensures a uniform sampling across the parameter space, even if the underlying distributions are non-uniform. We experiment with different numbers of quantiles (e.g., quartiles or quintiles) to optimize the balance between resolution and statistical power.

For higher-order analysis, we explore the use of two-dimensional binning (e.g., `A_SN1` vs. `A_AGN1`) to capture potential interactions between parameters (Cappellari & Copin 2002, 2003; Cappellari 2009). In cases where multi-dimensional binning leads to sparse bins, we employ regression techniques to disentangle the effects of individual parameters without excessive binning.

2.4. Calculation of Quenching Metrics and Uncertainty Estimation

For each combination of stellar mass bin and parameter bin, we calculate the quenched fraction (`f_quenched`), defined as the number of quenched galaxies (`N_quenched`) divided by the total number of galaxies

(N_{total}) within that bin (Xie et al. 2024).

$$f_{\text{quenched}} = \frac{N_{\text{quenched}}}{N_{\text{total}}} \quad (1)$$

In addition to the quenched fraction, we also compute the median sSFR within each bin to provide a continuous measure of star-forming activity (Banerjee et al. 2023; Shi et al. 2023).

To quantify the uncertainties associated with the quenched fraction and median sSFR, we employ a bootstrap resampling technique (Sanderson & Ponman 2009; Mohammad & Percival 2022). Within each bin, we resample galaxies with replacement a large number of times (e.g., 1000 times). For each resampled dataset, we recalculate the quenched fraction and median sSFR. The standard deviation of these resampled values is then used as an estimate of the uncertainty for each metric (Sanderson & Ponman 2009; Mohammad & Percival 2022).

2.5. Statistical Modeling and Regression Analysis

To quantify the dependence of quenching efficiency on feedback and cosmological parameters, we perform multivariate logistic regression (Kuschel et al. 2023; Xie et al. 2024; Rutkowski et al. 2025). The dependent variable is the quenched status of a galaxy (a binary variable indicating whether a galaxy is quenched or not), and the independent variables are the feedback parameters (A_{SN1} , A_{SN2} , A_{AGN1} , A_{AGN2}), the cosmological parameters (Ω_m , σ_8), and the logarithm of the stellar mass ($\log(M_{\text{star}})$). The logistic regression model takes the form:

$$\text{logit}(p) = \beta_0 + \beta_1 A_{\text{SN1}} + \beta_2 A_{\text{SN2}} + \beta_3 A_{\text{AGN1}} + \beta_4 A_{\text{AGN2}} + \beta_5 \Omega_m + \beta_6 \sigma_8 + \beta_7 \log(M_{\text{star}}) + \dots \quad (2)$$

where p is the probability of a galaxy being quenched, β_i are the regression coefficients, and the ellipsis indicates the potential inclusion of interaction terms (Romero-Gómez et al. 2024; Zheng et al. 2025).

We also consider the inclusion of interaction terms (e.g., $A_{\text{SN1}} \times A_{\text{AGN1}}$) in the regression model to capture potential non-linear effects and dependencies between parameters (Llorella & Cebrián 2025; Tian et al. 2025).

To isolate the direct effects of each parameter on the quenched fraction, we compute partial correlations between each parameter and the quenched fraction, controlling for stellar mass and the other parameters (Porrás-Valverde & Forbes 2024).

2.6. Model Validation and Robustness Checks

To assess the robustness of the regression results, we employ k-fold cross-validation (Hammond et al. 2024;

Sweet 2024). We divide the data into k folds (e.g., k=5) (Sweet 2024). For each fold, we fit the model on the remaining k-1 folds (the training set) and test its performance on the held-out fold (the testing set) (Sweet 2024). We repeat this process for each of the k folds, and record performance metrics such as accuracy and area under the receiver operating characteristic curve (AUC) (Hammond et al. 2024; Sweet 2024). The cross-validation provides an estimate of the model’s generalization performance and helps to prevent overfitting (Hammond et al. 2024; Sweet 2024).

We also perform robustness checks by repeating key analyses with alternative binning schemes (Leslie et al. 2021; Dainotti et al. 2024; Chen et al. 2024) and sSFR thresholds to confirm the stability of the results.

2.7. Computational Implementation

All data processing, analysis, and visualization are performed using Python, leveraging libraries such as `pandas`, `numpy`, `scikit-learn`, `matplotlib`, and `seaborn` (Giri 2025). Vectorized operations in `pandas` and `numpy` are used extensively to optimize computational efficiency (Turk & Smith 2011). For computationally intensive tasks such as bootstrap resampling and cross-validation, we leverage parallel processing using Python’s `concurrent.futures` module to utilize all available CPU cores (Turk & Smith 2011).

3. RESULTS

3.1. Quenched Fraction Trends

This section presents a detailed analysis of star formation quenching efficiency across the CAMELS simulation suite, focusing on the impact of supernova (SN) and active galactic nucleus (AGN) feedback parameters, as well as cosmological parameters. We explore trends in quenched fractions, examine the relative importance of each parameter using statistical modeling, and investigate the interplay between these factors in driving galaxy quenching at $z = 0$.

3.1.1. Stellar Mass Dependence

We begin by examining the quenched fraction (f_{quenched}), defined as the fraction of galaxies with specific star formation rate (sSFR) below 10^{-11} yr^{-1} , as a function of stellar mass and the varied simulation parameters. The distribution of sSFR for quenched and star-forming galaxies is shown in Figure 1, illustrating a clear separation between the two populations. The stellar mass distributions for quenched and star-forming galaxies are shown in Figure 2, indicating that star-forming galaxies tend to have lower stellar masses than quenched galaxies. Galaxies are binned into stellar mass ranges of width one dex.

A strong positive correlation exists between stellar mass and quenched fraction. In the highest mass bin considered, $10.5 \leq \log_{10}(M_{star}/M_{\odot}) < 11.5$, $f_{quenched}$ consistently exceeds 0.8 across all feedback parameter values. This indicates that galaxies in this mass range are nearly universally quenched, irrespective of the specific feedback implementation. In contrast, the quenched fraction varies significantly with feedback parameters in lower mass bins.

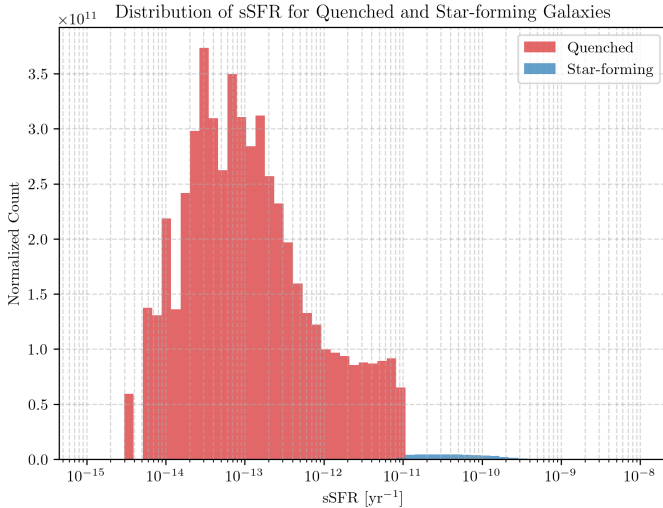


Figure 1. Distribution of specific star formation rates (sSFR) for quenched and star-forming galaxies. A clear separation is observed between the two populations, with quenched galaxies exhibiting significantly lower sSFR values compared to star-forming galaxies. The quenched galaxies have a higher normalized count at lower sSFR values.

3.1.2. Supernova Feedback

The parameter A_{SN1} , representing the SN wind energy per unit star formation rate, exhibits a notable *negative* correlation with $f_{quenched}$ in low to intermediate mass galaxies. This trend is illustrated in Figure 3, where the quenched fraction is plotted against A_{SN1} for different stellar mass bins. Specifically, for galaxies in the lowest mass bin ($9.5 \leq \log_{10}(M_{star}/M_{\odot}) < 10.5$), $f_{quenched}$ decreases from approximately 0.40 in the lowest quartile of A_{SN1} values to around 0.24 in the highest quartile. This suggests that enhanced SN feedback can suppress quenching, potentially by maintaining a turbulent interstellar medium (ISM) and preventing the collapse of gas clouds necessary for sustained star formation. The distribution of A_{SN1} for quenched and star-forming galaxies is shown in Figure 4, further highlighting the differences between the two populations.

3.1.3. AGN Feedback

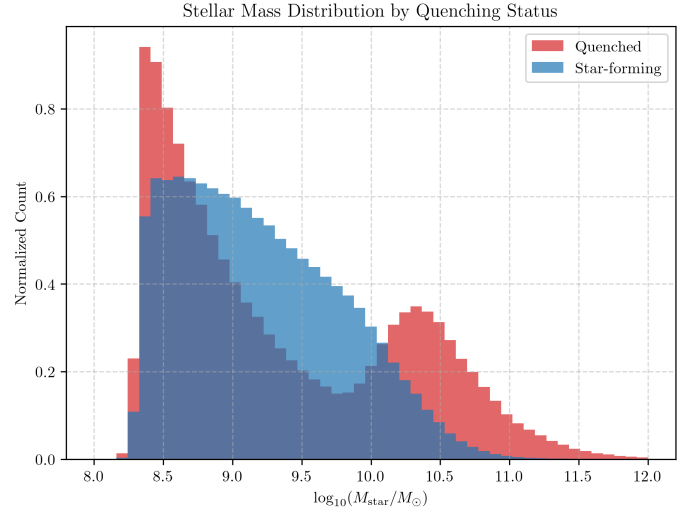


Figure 2. The figure shows the stellar mass distribution, separated by quenching status. The red histogram represents quenched galaxies, while the blue histogram represents star-forming galaxies. The x-axis shows the logarithm of the stellar mass in solar masses, and the y-axis shows the normalized count. There are large differences in the distributions, with star-forming galaxies peaking at lower stellar masses than quenched galaxies.

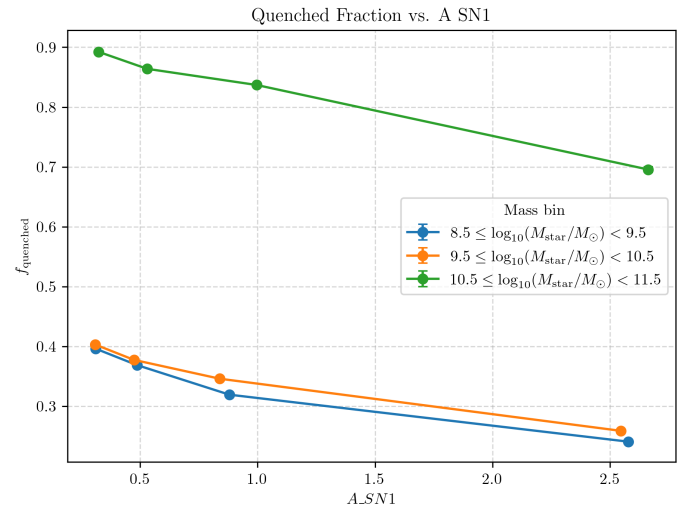


Figure 3. The figure shows the quenched fraction as a function of A_{SN1} for three different stellar mass bins: $8.5 \leq \log_{10}(M_{star}/M_{\odot}) < 9.5$, $9.5 \leq \log_{10}(M_{star}/M_{\odot}) < 10.5$, and $10.5 \leq \log_{10}(M_{star}/M_{\odot}) < 11.5$. The quenched fraction decreases with increasing A_{SN1} for all mass bins. At a given A_{SN1} , the quenched fraction is higher for more massive galaxies.

Conversely, the AGN feedback parameter A_{AGN1} , representing the AGN feedback energy per unit accretion rate, displays a positive correlation with $f_{quenched}$ across all mass bins. This trend is visible in Figure 5, which

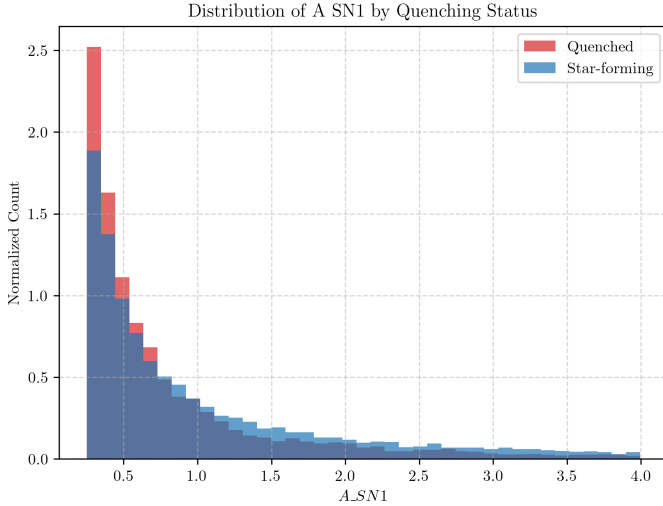


Figure 4. Distribution of A_{SN1} for quenched and star-forming galaxies. The plot shows the normalized count of A_{SN1} values, with quenched galaxies indicated in red and star-forming galaxies in blue. The distribution of A_{SN1} exhibits differences between the two types of galaxies.

shows the quenched fraction as a function of A_{AGN1} for different stellar mass bins. For example, in the highest mass bin, $f_{quenched}$ increases from approximately 0.72 in the lowest quartile of A_{AGN1} to approximately 0.94 in the highest quartile. Figure 6 shows the distribution of A_{AGN1} for quenched and star-forming galaxies, illustrating the higher A_{AGN1} values for quenched galaxies. This result supports the established paradigm that AGN feedback plays a critical role in maintaining quenching in massive galaxies, by heating and/or expelling the gas reservoir.

3.1.4. Other Feedback Parameters

The parameters A_{SN2} (SN wind speed) and A_{AGN2} (AGN kinetic mode ejection speed) show weaker and less systematic trends compared to A_{SN1} and A_{AGN1} . Figure 7 shows the quenched fraction as a function of A_{SN2} for different stellar mass bins, indicating a weak dependence. Similarly, Figure 9 shows the quenched fraction as a function of A_{AGN2} , also showing a weak dependence. The distributions of A_{SN2} and A_{AGN2} for quenched and star-forming galaxies are shown in Figure 8 and Figure 10, respectively. This suggests that the overall energy injected by feedback processes is more crucial for regulating quenching than the specific velocity of the outflows, at least within the parameter ranges explored in this study.

3.1.5. Cosmological Parameters

The cosmological parameters Ω_m (matter density parameter) and σ_8 (power spectrum normalization) also

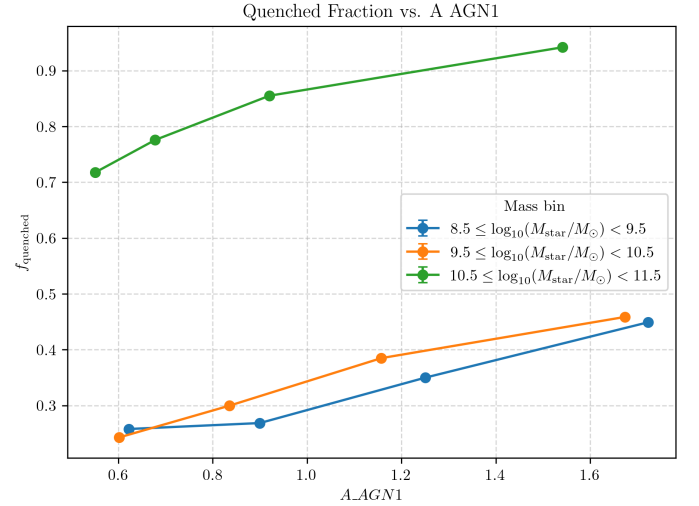


Figure 5. Quenched fraction as a function of A_{AGN1} for different stellar mass bins. The quenched fraction increases with increasing A_{AGN1} , with large differences seen between the different stellar mass bins.

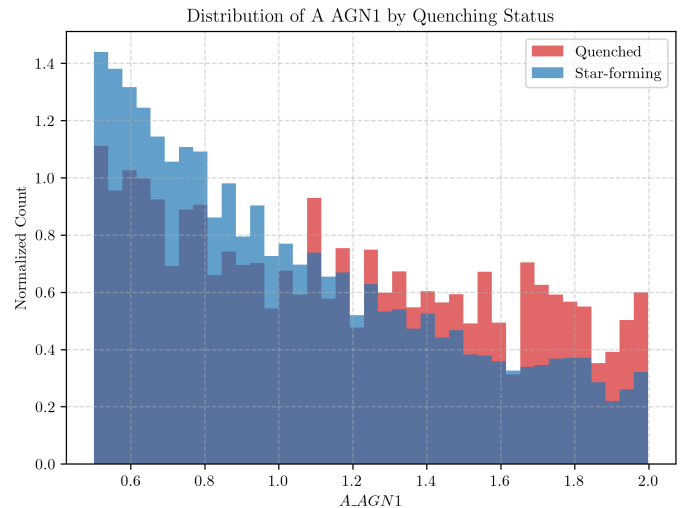


Figure 6. The distribution of A_{AGN1} is shown, separated by quenching status. Star-forming galaxies are shown in blue, while quenched galaxies are shown in red. There are large differences between the two populations with quenched galaxies having higher A_{AGN1} values.

influence the quenched fraction. Higher values of both parameters are associated with an increased $f_{quenched}$. This is consistent with the idea that denser cosmic environments and enhanced clustering, leading to earlier structure formation, favor quenching processes such as accelerated black hole growth and the formation of more massive halos, which more efficiently host quenching mechanisms.

3.2. Statistical Modeling and Feature Importance

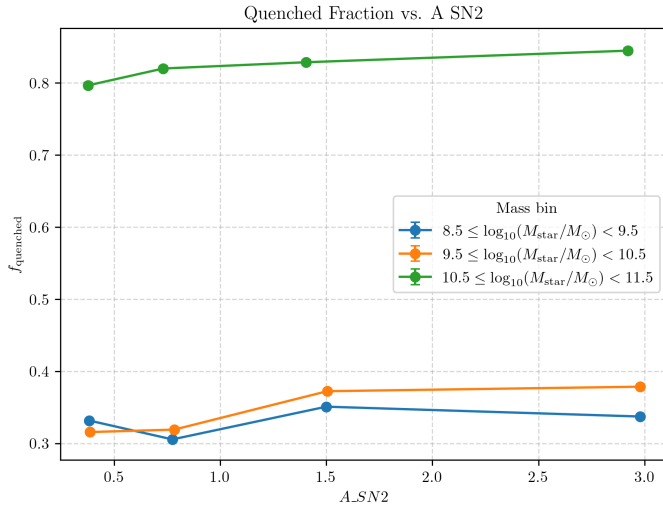


Figure 7. The figure displays the quenched fraction as a function of A_{SN2} for three different stellar mass bins. The quenched fraction increases with stellar mass, with galaxies in the highest mass bin ($10.5 \leq \log_{10}(M_{star}/M_{\odot}) < 11.5$) showing a consistently high quenched fraction across all values of A_{SN2} . The quenched fraction shows a weak dependence on A_{SN2} for each mass bin.

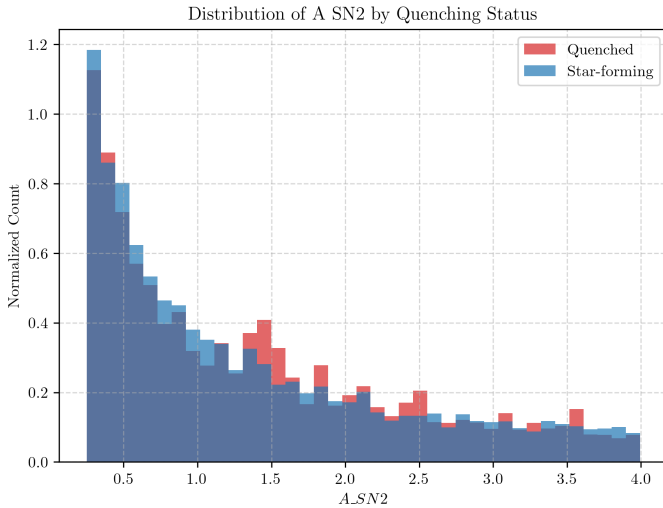


Figure 8. The distribution of A_{SN2} is shown for both quenched and star-forming galaxies. The distributions show that star-forming galaxies have a higher density at smaller A_{SN2} values than quenched galaxies.

To quantify the relative importance of each parameter in predicting galaxy quenching, we employ a logistic regression model. The target variable is a binary flag indicating whether a galaxy is quenched ($sSFR < 10^{-11} \text{ yr}^{-1}$). We use permutation feature importance to assess the contribution of each parameter to the model's performance.

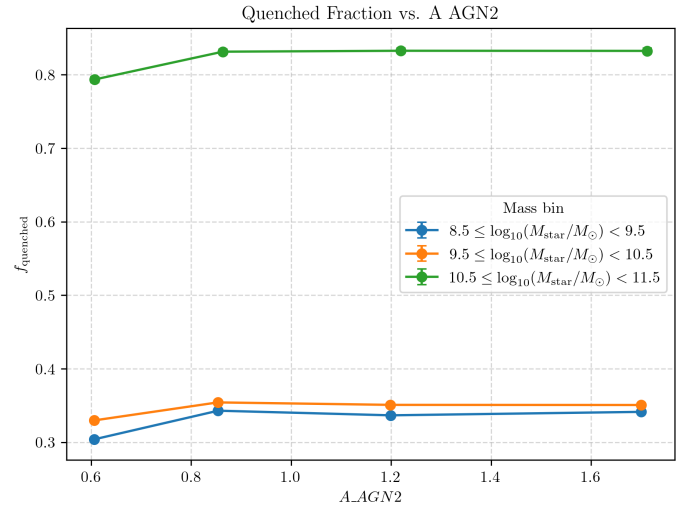


Figure 9. The quenched fraction as a function of A_{AGN2} for different stellar mass bins is shown. The quenched fraction is significantly higher for galaxies in the highest mass bin ($10.5 \leq \log_{10}(M_{star}/M_{\odot}) < 11.5$) compared to the lower mass bins. The quenched fraction appears to be relatively constant as a function of A_{AGN2} for each mass bin.

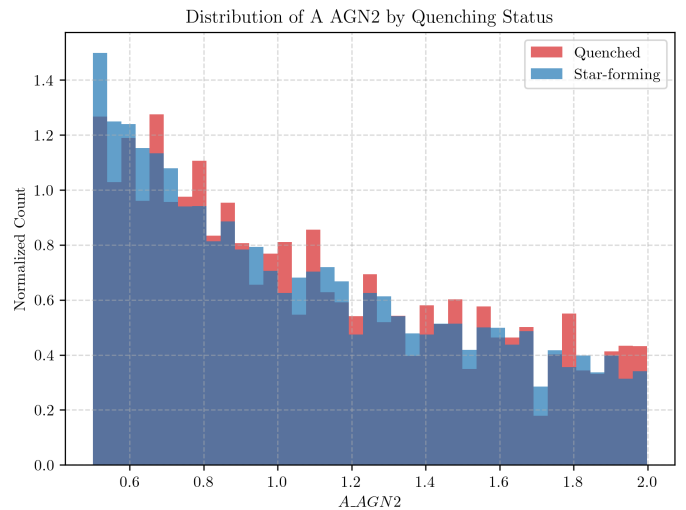


Figure 10. Distribution of A_{AGN2} for quenched and star-forming galaxies. The normalized count is plotted against A_{AGN2} . Overall, the star-forming galaxies tend to have slightly smaller A_{AGN2} values compared to quenched galaxies, but the differences are relatively small with significant overlap in the distributions.

3.2.1. Permutation Feature Importance

The permutation feature importance analysis reveals that σ_8 is the most important parameter (importance mean ~ 0.155), followed by A_{AGN1} (~ 0.148), Ω_m (~ 0.128), and the logarithm of stellar mass ($\log M_{star}$, ~ 0.104). The supernova feedback parameter A_{SN1} also

exhibits significant importance (~ 0.094). These results are summarized in Figure 11, which shows the permutation feature importances for all parameters. These results underscore the combined influence of cosmological environment, AGN feedback, and stellar mass on galaxy quenching.

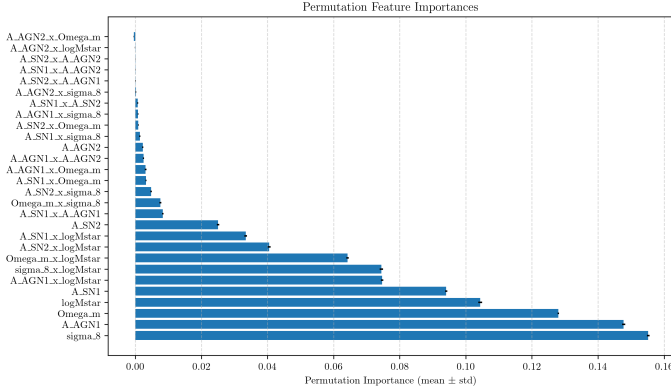


Figure 11. The figure displays the permutation feature importances, quantifying the contribution of different features and their combinations to the model’s performance. The x-axis represents the permutation importance (mean \pm std), while the y-axis lists the features. The features ”sigma_8”, ”A_AGN1”, ”Omega_m”, ”logMstar”, and ”A_SN1” show the largest permutation importance.

3.2.2. Logistic Regression Coefficients

The coefficients of the logistic regression model further highlight the key drivers of quenching. The coefficients are shown in Figure 12. A_{AGN1} has a strong positive coefficient (+1.87), indicating a strong positive association with quenching. Similarly, σ_8 (+1.66), $\log M_{star}$ (+1.41), and Ω_m (+1.13) also have positive coefficients. In contrast, A_{SN1} has a negative coefficient (-0.97), reflecting its role in suppressing quenching. The magnitudes of these coefficients emphasize the substantial impact of AGN feedback and cosmological parameters on driving galaxy quenching.

3.2.3. Partial Correlations

Partial correlation analysis, which measures the correlation between two variables while controlling for the effects of other variables, confirms the results obtained from the regression analysis. A_{AGN1} , σ_8 , and Ω_m exhibit positive partial correlations with quenching (with values around +0.15, +0.16, and +0.14, respectively), while A_{SN1} shows a negative partial correlation (-0.11).

3.2.4. Model Performance

The full logistic regression model, including all parameters and their interactions, achieves a mean accuracy

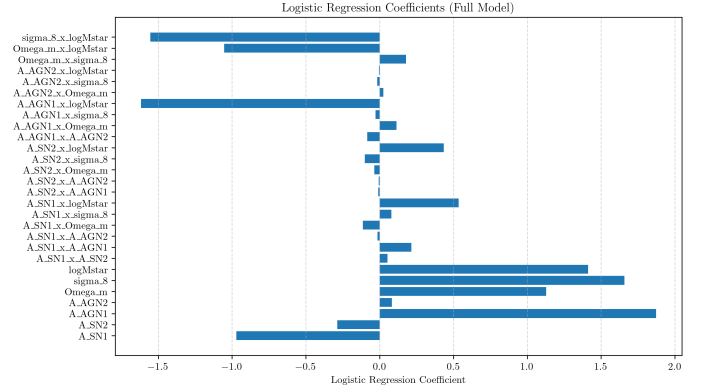


Figure 12. The figure shows the Logistic Regression Coefficients for the full model. Large differences are seen in the magnitude and sign of the coefficients, indicating varying degrees of influence from different combinations of cosmological parameters (e.g., σ_8 , Ω_m , $\log M_{star}$) and survey parameters (A_{SN1} , A_{SN2} , A_{AGN1} , A_{AGN2}) on the logistic regression model.

of approximately 66.5% and an area under the receiver operating characteristic curve (AUC) of approximately 0.685. A simplified model using only the top three most important features (σ_8 , A_{AGN1} , and Ω_m) yields slightly lower performance (accuracy $\sim 64.5\%$ and AUC ~ 0.645). This suggests that the majority of the predictive power is concentrated in a few key parameters, though the inclusion of other parameters does provide some additional predictive power.

3.3. Mass Dependence and Parameter Interplay

The analysis reveals that the dominant quenching mechanisms differ across stellar mass ranges. AGN feedback appears to be the primary driver of quenching in high-mass galaxies, while SN feedback plays a more regulatory role in low to intermediate mass systems.

To further explore the interplay between parameters, we generate two-dimensional heatmaps showing the quenched fraction as a function of pairs of parameters. Figure 13 shows the heatmap of the quenched fraction as a function of A_{AGN1} and A_{SN1} for galaxies with stellar masses in the range $8.5 \leq \log_{10}(M_{star}/M_{\odot}) < 9.5$. Figure 14 and Figure 15 show the same heatmap for galaxies with stellar masses in the range $9.5 \leq \log_{10}(M_{*}/M_{\odot}) < 10.5$ and $10.5 \leq \log_{10}(M_{*}/M_{\odot}) < 11.5$, respectively. These visualizations indicate that the highest quenched fractions occur in regions where A_{AGN1} is high and A_{SN1} is low. This suggests a synergistic effect, where quenching is most efficient when AGN feedback is strong and SN feedback is weak. This also suggests that the quenching is not simply a linear combination of the effects of the parameters, but that there are non-linear interactions between them.

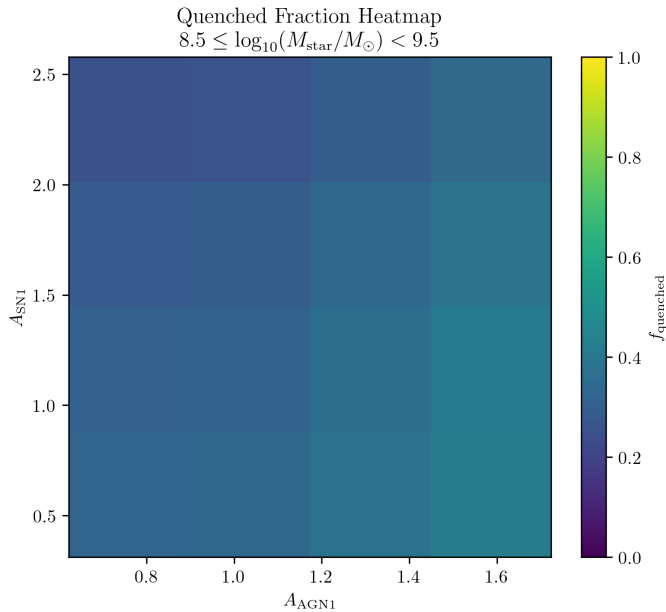


Figure 13. Heatmap of the quenched fraction (f_{quenched}) as a function of A_{AGN1} and A_{SN1} for galaxies with stellar masses in the range $8.5 \leq \log_{10}(M_{\text{star}}/M_{\odot}) < 9.5$. The quenched fraction increases with increasing A_{AGN1} and *decreasing* A_{SN1} , with a more pronounced increase along the A_{AGN1} axis.

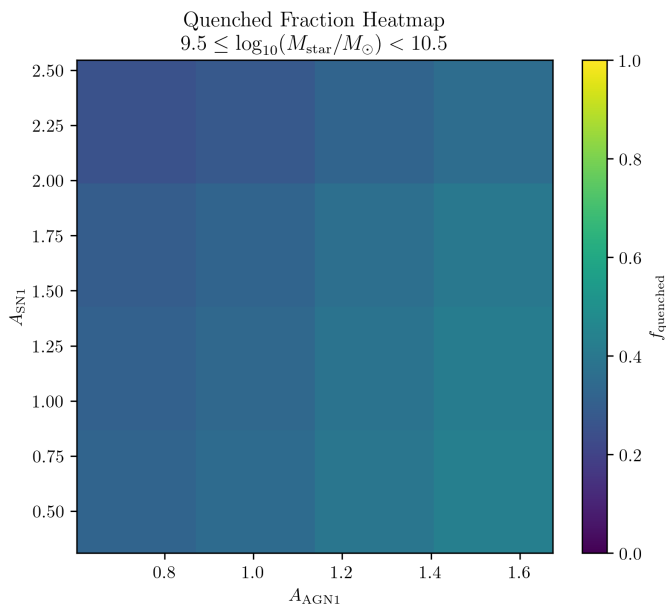


Figure 14. Quenched fraction heatmap for galaxies with stellar masses in the range $9.5 \leq \log_{10}(M_{\star}/M_{\odot}) < 10.5$. The x-axis represents A_{AGN1} and the y-axis represents A_{SN1} . The colorbar indicates the quenched fraction, f_{quenched} . The quenched fraction increases as you move towards larger values of A_{AGN1} .

4. CONCLUSIONS

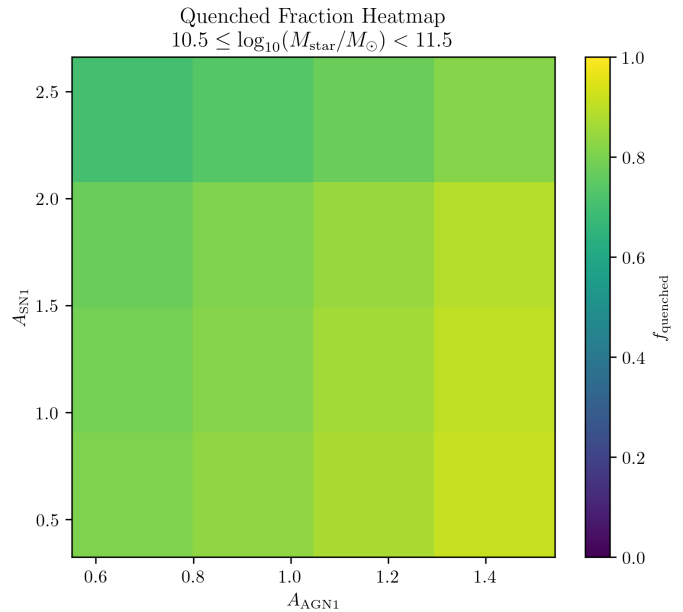


Figure 15. Quenched fraction of galaxies with stellar mass $10.5 \leq \log_{10}(M_{\star}/M_{\odot}) < 11.5$ as a function of A_{AGN1} and A_{SN1} . The quenched fraction increases with increasing A_{AGN1} .

In this study, we have systematically investigated the efficiency of star formation quenching across a wide range of feedback and cosmological parameters using the CAMELS simulations. Our primary goal was to disentangle the complex interplay between supernova (SN) feedback, active galactic nucleus (AGN) feedback, and cosmological parameters in driving the cessation of star formation in galaxies at $z = 0$. By leveraging the extensive parameter space coverage of the CAMELS simulations, we aimed to provide quantitative insights into the physical drivers of quenching and offer predictive guidance for galaxy evolution models and future observational surveys.

We utilized galaxy-level data from the IllustrisTNG and SIMBA simulation suites within CAMELS, focusing on key parameters such as SN feedback efficiency (A_{SN1} , A_{SN2}), AGN feedback efficiency (A_{AGN1} , A_{AGN2}), matter density parameter (Ω_m), and the amplitude of the matter power spectrum (σ_8). We calculated the quenched fraction (f_{quenched}) for galaxies in different stellar mass bins and explored the dependence of f_{quenched} on the aforementioned parameters. Statistical techniques, including permutation feature importance, logistic regression, and partial correlation analysis, were employed to quantify the relative importance of each parameter and to uncover potential interactions.

Our results reveal a nuanced picture of galaxy quenching. We found that AGN feedback, particularly the

AGN feedback energy per accretion (A_{AGN1}), is the dominant quenching mechanism in massive galaxies, while SN feedback exhibits a more regulatory effect in lower-mass systems. Specifically, an increase in A_{AGN1} correlates with a higher quenched fraction, especially in galaxies with $\log_{10}(M_{star}/M_{\odot}) \geq 10.5$. Conversely, higher SN wind energy (A_{SN1}) tends to *decrease* the quenched fraction in low to intermediate mass galaxies. Furthermore, we observed that cosmological parameters (Ω_m and σ_8) positively influence quenching efficiency, suggesting that denser cosmic environments and enhanced clustering promote quenching.

From this study, we have learned that the efficiency of star formation quenching is not solely determined by internal feedback processes but is also significantly influenced by the broader cosmological context. The interplay between AGN feedback, SN feedback, and cosmological parameters is complex and nonlinear, with stellar

mass acting as a crucial modulator. Our findings underscore the importance of accurately representing AGN feedback in galaxy evolution models, particularly for massive galaxies, and of considering the environmental context when studying quenching. The results also suggest that future models should adopt a joint, nonlinear approach to capture the synergistic effects that operate across different mass regimes.

In conclusion, our analysis of the CAMELS simulations provides a comprehensive map of star formation quenching efficiency across feedback and cosmological parameter space. We have demonstrated that AGN feedback, SN feedback, and cosmological parameters all play significant, interconnected roles in driving the cessation of star formation in galaxies. These findings offer valuable insights for refining galaxy evolution models and interpreting observational data from future surveys.

REFERENCES

- Arango-Toro, R. C., Ilbert, O., Ciesla, L., et al. 2025, COSMOS-Web: A history of galaxy migrations over the stellar mass-star formation rate plane, doi: <https://doi.org/10.1051/0004-6361/202452519>
- Banerjee, A., Pandey, B., & Nandi, A. 2023, Clustering and physical properties of the star-forming galaxies and AGN: does assembly bias have a role in AGN activity? <https://arxiv.org/abs/2310.12943>
- Bauer, A. E., Drory, N., & Hill, G. J. 2005, Specific Star Formation Rates. <https://arxiv.org/abs/astro-ph/0509059>
- Bluck, A. F. L., Piotrowska, J. M., & Maiolino, R. 2023, The fundamental signature of star formation quenching from AGN feedback: A critical dependence of quiescence on supermassive black hole mass not accretion rate, doi: <https://doi.org/10.3847/1538-4357/acac7c>
- Bravo, M., Robotham, A. S. G., del P. Lagos, C., et al. 2023, Galaxy quenching timescales from a forensic reconstruction of their colour evolution, doi: <https://doi.org/10.1093/mnras/stad1234>
- Cappellari, M. 2009, Voronoi binning: Optimal adaptive tessellations of multi-dimensional data. <https://arxiv.org/abs/0912.1303>
- Cappellari, M., & Copin, Y. 2002, Adaptive Spatial Binning of 2D Spectra and Images Using Voronoi Tessellations. <https://arxiv.org/abs/astro-ph/0202379>
- . 2003, Adaptive spatial binning of integral-field spectroscopic data using Voronoi tessellations, doi: <https://doi.org/10.1046/j.1365-8711.2003.06541.x>
- Carr, C., Bryan, G. L., Fielding, D. B., Pandya, V., & Somerville, R. S. 2022, Regulation of Star Formation by a Hot Circumgalactic Medium, doi: <https://doi.org/10.3847/1538-4357/acc4c7>
- Chen, C. M. H., Arnaud, M., Pointecouteau, E., Pratt, G. W., & Iqbal, A. 2024, Evolution of X-ray galaxy Cluster Properties in a Representative Sample (EXCPreS). Optimal binning for temperature profile extraction, doi: <https://doi.org/10.1051/0004-6361/202348411>
- Comparat, J., Merloni, A., Ponti, G., et al. 2025, Cross-correlation between soft X-rays and galaxies A new benchmark for galaxy evolution models. <https://arxiv.org/abs/2503.19796>
- Contardo, G., Trotta, R., Gioia, S. D., Hogg, D. W., & Villaescusa-Navarro, F. 2025, On the effects of parameters on galaxy properties in CAMELS and the predictability of Ω_m . <https://arxiv.org/abs/2503.22654>
- Dainotti, M. G., Lenart, A. L., Yengejeh, M. G., et al. 2024, A new binning method to choose a standard set of Quasars. <https://arxiv.org/abs/2401.12847>
- Das, A., Pandey, B., & Sarkar, S. 2023, Galaxy interactions in filaments and sheets: insights from EAGLE simulations, doi: <https://doi.org/10.1088/1674-4527/acf6f5>
- Das, A., Pandey, B., Sarkar, S., & Dutta, A. 2021, Galaxy interactions in different environments: An analysis of galaxy pairs from the SDSS. <https://arxiv.org/abs/2108.05874>

- de Santi, N. S. M., Villaescusa-Navarro, F., Abramo, L. R., et al. 2025, Field-level simulation-based inference with galaxy catalogs: the impact of systematic effects, doi: <https://doi.org/10.1088/1475-7516/2025/01/082>
- Dou, J., Peng, Y., Gu, Q., et al. 2025, The critical role of dark matter halos in driving star formation. <https://arxiv.org/abs/2503.04243>
- Ellison, S. L., Ferreira, L., Wild, V., et al. 2024, Galaxy evolution in the post-merger regime. II – Post-merger quenching peaks within 500 Myr of coalescence, doi: <https://doi.org/10.33232/001c.127779>
- Geha, M., Mao, Y.-Y., Wechsler, R. H., et al. 2024, The SAGA Survey. IV. The Star Formation Properties of 101 Satellite Systems around Milky Way-mass Galaxies, doi: <https://doi.org/10.3847/1538-4357/ad61e7>
- Giri, S. K. 2025, AstronomyCalc: A python toolkit for teaching Astronomical Calculations and Data Analysis methods. <https://arxiv.org/abs/2501.05491>
- Hammond, M., Lewis, N. T., Boone, S., et al. 2024, Identifying and Fitting Eclipse Maps of Exoplanets with Cross-Validation. <https://arxiv.org/abs/2405.20689>
- Hopkins, P. F., Quataert, E., & Murray, N. 2011, Self-Regulated Star Formation in Galaxies via Momentum Input from Massive Stars, doi: <https://doi.org/10.1111/j.1365-2966.2011.19306.x>
- Ivanov, M. M., Obuljen, A., Cuesta-Lazaro, C., & Toomey, M. W. 2025, Full-shape analysis with simulation-based priors: cosmological parameters and the structure growth anomaly. <https://arxiv.org/abs/2409.10609>
- Katsianis, A., Xu, H., Yang, X., et al. 2020, The specific star formation rate function at different mass scales and quenching: A comparison between cosmological models and SDSS, doi: <https://doi.org/10.1093/mnras/staa3236>
- Kurinci-Vendhan, S., Farcy, M., Hirschmann, M., & Valentino, F. 2024, On the origin of star formation quenching in massive galaxies at $z \gtrsim 3$ in the cosmological simulations IllustrisTNG, doi: <https://doi.org/10.1093/mnras/stae2297>
- Kuschel, M., Scarlata, C., Mehta, V., et al. 2023, Investigating the Dominant Environmental Quenching Process in UVCANDELS/COSMOS Groups, doi: <https://doi.org/10.3847/1538-4357/acacfd>
- Lapi, A., Boco, L., & Shankar, F. 2025, Semi-empirical Models of Galaxy Formation and Evolution. <https://arxiv.org/abs/2502.12764>
- Lee, M. E., Genel, S., Wandelt, B. D., et al. 2024, Zooming by in the CARPoolGP lane: new CAMELS-TNG simulations of zoomed-in massive halos. <https://arxiv.org/abs/2403.10609>
- Leslie, N., Dai, L., & Pratten, G. 2021, Mode-by-mode Relative Binning: Fast Likelihood Estimation for Gravitational Waveforms with Spin-Orbit Precession and Multiple Harmonics, doi: <https://doi.org/10.1103/PhysRevD.104.123030>
- Leslie, S., Schinnerer, E., Liu, D., et al. 2020, The VLA-COSMOS 3 GHz Large Project: Evolution of specific star formation rates out to $z \sim 5$, doi: <https://doi.org/10.3847/1538-4357/aba044>
- Li, F., Rahman, M., Murray, N., et al. 2024a, The Effect of Galaxy Interactions on Starbursts in Milky Way-Mass Galaxies in FIRE Simulations. <https://arxiv.org/abs/2411.10373>
- Li, Y. Q., Do, T., Jones, E., et al. 2024b, Using Galaxy Evolution as Source of Physics-Based Ground Truth for Generative Models. <https://arxiv.org/abs/2407.07229>
- Llorella, F. R., & Cebrián, J. A. 2025, Exploring symbolic regression and genetic algorithms for astronomical object classification, doi: <https://doi.org/10.33232/001c.132333>
- Mao, Z., Kodama, T., Pérez-Martínez, J. M., et al. 2022, Revealing impacts of stellar mass and environment on galaxy quenching, doi: <https://doi.org/10.1051/0004-6361/202243733>
- Martin, W., & Mortlock, D. J. 2024, Robust Bayesian regression in astronomy. <https://arxiv.org/abs/2411.02380>
- Mohammad, F. G., & Percival, W. J. 2022, Creating Jackknife and Bootstrap estimates of the covariance matrix for the two-point correlation function, doi: <https://doi.org/10.1093/mnras/stac1458>
- Mucesh, S., Hartley, W. G., Gilligan-Lee, C. M., & Lahav, O. 2024, Nature versus nurture in galaxy formation: the effect of environment on star formation with causal machine learning. <https://arxiv.org/abs/2412.02439>
- Narkedimilli, S., Raghav, S., Makam, S., Ayitapu, P., & H, A. B. 2024, Predicting Stellar Metallicity: A Comparative Analysis of Regression Models for Solar Twin Stars. <https://arxiv.org/abs/2410.06709>
- Piotrowska, J. M., Bluck, A. F. L., Maiolino, R., & Peng, Y. 2021, On the quenching of star formation in observed and simulated central galaxies: Evidence for the role of integrated AGN feedback, doi: <https://doi.org/10.1093/mnras/stab3673>
- Porrás-Valverde, A. J., & Forbes, J. C. 2024, On the signature of black holes on the quenched stellar mass function. <https://arxiv.org/abs/2412.04553>
- Pérez-Millán, D., Fritz, J., González-Lópezlira, R. A., et al. 2023, The relation between morphology, star formation history, and environment in local universe galaxies, doi: <https://doi.org/10.1093/mnras/stad542>

- Romero-Gómez, J., Peletier, R. F., Aguerri, J. A. L., & Smith, R. 2024, Are early-type galaxies quenched by present-day environment? A study of dwarfs in the Fornax Cluster, doi: <https://doi.org/10.1051/0004-6361/202348530>
- Rutkowski, M. J., Zabelle, B., Hagen, T., et al. 2025, Recent star formation in $0.5 < z < 1.5$ quiescent galaxies, doi: <https://doi.org/10.3847/2041-8213/adbe7c>
- Sanderson, A. J. R., & Ponman, T. J. 2009, X-ray modelling of galaxy cluster gas and mass profiles, doi: <https://doi.org/10.1111/j.1365-2966.2009.15888.x>
- Schawinski, K., Turp, M. D., & Zhang, C. 2018, Exploring galaxy evolution with generative models, doi: <https://doi.org/10.1051/0004-6361/201833800>
- Shi, K., Malavasi, N., Toshikawa, J., & Zheng, X. 2023, Nature vs. Nurture: Revisiting the environmental impact on star formation activities of galaxies. <https://arxiv.org/abs/2311.18427>
- Stoppa, F., Cator, E., & Nelemans, G. 2023, Consistency Tests for Comparing Astrophysical Models and Observations, doi: <https://doi.org/10.1093/mnras/stad1938>
- Subramanian, S., Mondal, C., & Kalari, V. 2023, Effect of low-mass galaxy interactions on their star formation, doi: <https://doi.org/10.1051/0004-6361/202346536>
- Sweet, A. 2024, Predicting Exoplanetary Features with a Residual Model for Uniform and Gaussian Distributions. <https://arxiv.org/abs/2406.10771>
- Tian, Y., Zhou, W., Viscione, M., et al. 2025, Interactive Symbolic Regression through Offline Reinforcement Learning: A Co-Design Framework. <https://arxiv.org/abs/2502.02917>
- Turk, M. J., & Smith, B. D. 2011, High-Performance Astrophysical Simulations and Analysis with Python. <https://arxiv.org/abs/1112.4482>
- Vaughan, S. P., van de Sande, J., Fraser-McKelvie, A., et al. 2024, The SAMI galaxy survey: predicting kinematic morphology with logistic regression. <https://arxiv.org/abs/2402.03676>
- Villaescusa-Navarro, F., Genel, S., Anglés-Alcázar, D., et al. 2022, The CAMELS project: public data release, doi: <https://doi.org/10.3847/1538-4365/acbf47>
- Whitaker, K. E., Bezanson, R., van Dokkum, P. G., et al. 2017, Predicting Quiescence: The Dependence of Specific Star Formation Rate on Galaxy Size and Central Density at $0.5 < z < 2.5$, doi: <https://doi.org/10.3847/1538-4357/aa6258>
- Wijesinghe, D. B., Hopkins, A. M., Brough, S., et al. 2012, Galaxy And Mass Assembly (GAMA): Galaxy environments and star formation rate variations, doi: <https://doi.org/10.1111/j.1365-2966.2012.21164.x>
- Xie, L., Lucia, G. D., Fontanot, F., et al. 2024, The first quenched galaxies, when and how? <https://arxiv.org/abs/2402.01314>
- Zheng, Y., Xu, K., Zhao, D., et al. 2025, Photometric Objects Around Cosmic Webs (PAC). VII. Disentangling Mass and Environment Quenching with the Aid of Galaxy-halo Connection in Simulations. <https://arxiv.org/abs/2501.00986>